ISSN: 2277-9655
Impact Factor: 1.852

IJESRT

INTERNATIONAL JOURNAL OF ENGINEERING SCIENCES & RESEARCH TECHNOLOGY

Impact of RZ Duty-Cycle, Dispersion Map and Nonlinearity on the Performance of 107Gbps OOK Transmission over 1000 km SSMF

Aras Saeed Mahmood[*1], Ghafour Amouzad Mahdiraji[2], Ahmad Fauzi Abas[3]
[*1]Department of Physics, University of Sulaimani, Kurdistan Region, Iraq
[2,3]Photonics and Fiber Optic Systems Laboratory, Centre of Excellence for Wireless and Photonics Networks, Engineering and Technology Complex, University Putra Malaysia, 43400 Serdang, Selangor, Malaysia
arasmahmud957@yahoo.com

Abstract

The effect of the dispersion map and nonlinearity on performance of 107 Gbps on-off-keying with different return-to-zero duty-cycle over long-haul transmission is investigated by simulation. It is observed that without existence of nonlinearity, different dispersion maps perform almost similar. However, performance difference between different dispersion maps becomes noticeable when nonlinearity presents in the system. In existence of nonlinearity, at any launched power, the map with around 10% dispersion pre- and 90% post-compensation shows the optimum performance.

Keywords: Optical fiber communication; return-to-zero duty-cycle; on-off-keying (OOK); dispersion compensation; symmetric dispersion map; nonlinearity

Introduction

In ultrafast optical transmission system, chromatic dispersion plays as the main factor that limits the transmission distance (Wang et al., 2010, Jansen et al., 2007, Schubert et al., 2007, Milivojevic et al., 2005, Takiguchi et al., 1998). In single wavelength long-haul transmission the interaction between self- phase modulation (SPM) and group velocity dispersion (GVD) causes severe waveform distortion (Jain and Kumar, 2010, Malekmohammadi et al., 2009). An effective approach to minimize the accumulation of nonlinear distortion along optical links is the optimization of the cumulated dispersion profile, commonly referred to as dispersion map (Fischer et al., 2009, Bo-ning et al., 2010, Frignac and Ramantanis, 2010, Huang et al., 2010, Supradeepa et al., 2010, Xuejun et al., 2010, Zhang-Di et al., 2010). The map, which uses distributed in-line dispersion compensation instead of lumped compensation at the receiver or the transmitter, is quite effective in suppressing the SPM–GVD interaction (Jain and Kumar, 2010). In addition, by simulation, it has been shown that symmetric dispersion compensation in long-haul transmission provides lower signal degradation compared to asymmetric maps (Mu and Menyuk, 2001).

Different modulation formats had been used for long-haul transmission systems (Abas et al., 2007, Cho et al., 2003, Taga and Chung, 2010). However, intensity modulation with direct detection is still the most popularly employed techniques due to its simplicity and lower implementation cost. At bit rates of 10Gbps and higher, it has been shown that return-to-zero (RZ) offers superior performance over non return-to-zero (NRZ) in certain regimes where chromatic dispersion and fiber nonlinearities are present (Ip and Kahn, 2006, Jopson et al., 1999, Mu and Menyuk, 2001). In this paper, the impact of eleven different symmetric dispersion maps and different launched power on the performance of 107 Gp/s on-off keying (OOK) with 33%, 50%, and 67% RZ duty-cycles over 1000 km standard single mode fiber (SSMF) is investigated.

Simulation Model

Figure 1 shows the schematic diagram of the simulation model. The simulation is conducted by using the established commercial software named OptiSystem. At the transmitter side, an RZ signal generator is used to produce 107 Gbps bit streams with 2^{10}-1 pseudo random binary signal (PRBS). In this study, three different RZ duty-cycles, i.e. 33%, 50% and 67%, are used to investigate the duty cycle impacts on the performance of the system. The output of the RZ pulse generator is then externally modulated over an optical carrier using Mach-Zehnder Modulator (MZM) with 30 dB extinction ratio. The optical carrier signal is generated from a distributed feedback (DFB) laser diode (LD), operating at 1550 nm.

ISSN: 2277-9655
Impact Factor: 1.852

The modulated signal is then transmitted over ten 100 km span, which result in a total of 1000 km SSMF. Each SSMF span contains 1675 ps/nm of chromatic dispersion. The detail specification is shown in Table 1. The total dispersion per SSMF is compensated by 16.75 km DCF with dispersion coefficient of –100 ps/(nm·km). The dispersion compensation per SSMF is performed in eleven different symmetric maps (Table 2). For the first map, the total dispersion of SSMF is compensated using 16.75 km DCF located after each SSMF span as post-compensation. In the second map, 10% of total dispersion of SSMF, i.e. 167.5 ps/nm, is compensated using 1.675 km DCF located before every SSMF span as the pre-compensation, and the balance of 90%, i.e. 1507.5 ps/nm, is compensated by 15.075 km DCF located after each SSMF span as post-compensation. As shown in Table 2, for the following map, the amount of dispersion compensated as pre-compensation is increased by 10%, while the amount of post-compensation is reduced by 10%. Finally, in the map 11, the total dispersion per SSMF, i.e., 1675 ps/nm is compensated using 16.75 km DCF located before every SSMF span as pre-compensation. For all dispersion maps, there should be 16.75 km DCF that act as the in-line-DCF, between every two adjacent SSMF span in the link.

The total loss per SSMF is compensated by Erbium doped fiber amplifier (EDFA) with 4 dB noise figure and identical gain. The launched power into every SSMF and DCF is controlled by using an optical attenuator located after every EDFA. In this study, fifteen different combinations of launched power into SSMF and DCF are investigated, which consist of three different launched powers into SSMFs, i.e., +5, +7, and +9 dBm, and five different launched powers into DCFs, i.e., –4.5, –3, –1.5, –0, and +1.5 dBm. At the receiver side, a Gaussian optical band-pass filter (BPF) with 100 GHz cut-off frequency is used to eliminate the system noise that mainly produced by optical amplifiers. Then the received optical signal is detected by a p-i-n photodiode (PD) followed by a low-pass filter (LPF). The launched power into the PD is controlled by an optical attenuator located before the BPF to assure the power reaching the photodiode not exceed the limit. Cut-off frequency of the electrical Gaussian LPF is set at 64.2 GHz to minimize the PD noise. Performance of the received signal after the LPF is evaluated from the signal eye diagrams.

Results and Discussion

Figure 2 shows the performance of 107 Gb/s OOK over eleven different dispersion map. Figures 2 (a1), (b1), (c1), (d1) and (e1) present the performance of RZ signal with 33% duty-cycle for the case that the launched power into DCFs is set at –4.5, –3, –1.5, 0, and +1.5 dBm, respectively. In general, when the launched power into SSMF is as low as +5 dBm, almost similar performance is observed over different dispersion maps. At the same power into SSMF, by increasing the launched power into DCF from –4.5 to +1.5 dBm the Q-factor improves from around 4 to around 5. This improvement is due to the increment in optical signal to noise ratio (OSNR). In addition, it shows that the nonlinearity is not yet pronounced.

By increasing the launched power into SSMF to +7 dBm, the performance of the system at the lower launched power into DCF is improved, however, starts to degrade at the higher launched power. At launched power of +9 dBm into SSMF, the nonlinearity of the system started to rise, which made the system performance severely affected in some dispersion maps. This can be clearly witnessed when high pre-compensation value involves. Thus, in general, at the lower power, all dispersion maps have almost similar performance, however, performance difference between different maps become more significant when nonlinearity exist in the system due to the high launched power. This is due to the interaction between the SPM and GVD, which is constructive in the map with post-compensation; while destructive in the pre-compensation map. Similar results are observed for the RZ signals with 50% and 67% duty-cycle. The only difference is that the nonlinearity starts at the lower power compared to 33%. This is due to the higher amount of power contained in the RZ signal with the larger duty-cycle. The results show that selecting an appropriate dispersion map for RZ with larger duty-cycle is more important especially if launched power into the system is high. In general, the results in Figures 2 show that when the nonlinearity presents in the system due to the high amount of power, the most optimum dispersion map is 10% pre-compensation and 90% post-compensation. In this dispersion map, the interaction between SPM and GVD is effectively constructive.

Figure 3 shows examples of the eye diagrams selected for the case that the launched power into DCFs and SSMFs are –3 and +9 dBm, respectively. Figures 3(a), (b), and (c) show the eye diagrams for 33%, 50%, and 67% RZ for the case of 10% dispersion pre-compensation, respectively. The eye diagrams show that 33% RZ (Q-factor=4.5) has very clear eye opening as compared to 50% RZ (Q-factor=3.7). For 67% RZ the eye is fully closed due to the high nonlinear effect. Eye diagrams of 33%, 50% and 67% RZ at 40%, 30% and 20% dispersion pre-compensation is shown in Figures 3(d), (e), and (f), respectively. Even though all the three eyes in this case have the Q-factor of around 0, the eye

ISSN: 2277-9655
Impact Factor: 1.852

diagrams suggest that 33% RZ has a better quality as compared to 50%. In comparison to 67% RZ, both 33% and 50% have relatively better quality eye.

Conclusion

Transmission performance of 107 Gbps RZ signal with three different duty-cycles over 1000 km SSMF with 11 different dispersion maps was investigated. At the lower launched power or shorter RZ duty-cycle, all dispersion maps show almost similar performance. However, performance difference between different dispersion maps rises when nonlinearity presents in the system. In overall, in existence of nonlinearity, around 10% dispersion pre- and 90% post-compensation realized the best dispersion map. In addition, RZ signal with the shorter duty-cycle is more resilient to dispersion. The output from this research can be used as dispersion management guideline for high-bit rate long-haul transmission system.

References

[1] ABAS, A. F., HIDAYAT, A., SANDEL, D., MILIVOJEVIC, B. & NOE, R. (2007) 100 km fiber span in 292 km, 2.38 Tb/s (16×160 Gb/s) WDM DQPSK polarization division multiplex transmission experiment without Raman amplification. Optical Fiber Technology, 13, 46-50.

[2] BO-NING, H., WANG, J., WANG, W. & RUI-MEI, Z. (2010) Analysis on dispersion compensation with DCF based on Optisystem. Industrial and Information Systems (IIS), 2010 2nd International Conference on.

[3] CHO, P. S., GRIGORYAN, V. S., GODIN, Y. A., SALAMON, A. & ACHIAM, Y. (2003) Transmission of 25-Gb/s RZ-DQPSK signals with 25-GHz channel spacing over 1000 km of SMF-28 fiber. Photonics Technology Letters, IEEE, 15, 473-475.

[4] FISCHER, J. K., BUNGE, C. A. & PETERMANN, K. (2009) Equivalent single-span model for dispersion-managed fiber-optic transmission systems. Journal of Lightwave Technology, 27, 3425-3432.

[5] FRIGNAC, Y. & RAMANTANIS, P. (2010) Average Optical Phase Shift as an Indicator of the Dispersion Management Optimization in PSK-Modulated Transmission Systems. Photonics Technology Letters, IEEE, 22, 1488-1490.

[6] HUANG, L., SONG, X., LIU, F., SHEN, L. & HAN, L. (2010) Computer simulation of 40Gb/s optical fiber transmission systems with a fiber grating dispersion compensator. Computer Design and Applications (ICCDA), 2010 International Conference on.

[7] IP, E. & KAHN, J. M. (2006) Power spectra of return-to-zero optical signals. Journal of Lightwave Technology, 24, 1610-1618.

[8] JAIN, B. & KUMAR, M. (2010) Simulative analysis of pre- and post-compensation using CRZ format in WDM optical transmission link. Optik, 121, 1948-1954.

[9] JANSEN, S. L., DERKSEN, R. H., SCHUBERT, C., ZHOU, X., BIRK, M., WEISKE, C. J., BOHN, M., VAN DEN BORNE, D., KRUMMRICH, P. M., MOLLER, M., HORST, F., OFFREIN, B. J., DE WAARDT, H., KHOE, G. D. & KIRSTADTER, A. (2007) 107-Gb/s full-ETDM transmission over field installed fiber using vestigial sideband modulation. Optical Fiber Communication and the National Fiber Optic Engineers Conference, 2007. OFC/NFOEC 2007. Conference on.

[10] JOPSON, R. M., NELSON, L. E., PENDOCK, G. J. & GNAUCK, A. H. (1999) Polarization-mode dispersion impairment in return-to-zero and nonreturn-to-zero systems. Optical Fiber Communication Conference, 1999, and the International Conference on Integrated Optics and Optical Fiber Communication. OFC/IOOC '99. Technical Digest.

[11] MALEKMOHAMMADI, A., MAHDIRAJI, G. A., ABAS, A. F., ABDULLAH, M. K., MOKHTAR, M. & RASID, M. F. A. (2009) Effect of self-phase-modulation on dispersion compensated absolute polar duty cycle division multiplexing Transmission. IET Optoelectronics, 3, 207-214.

[12] MILIVOJEVIC, B., ABAS, A. F., HIDAYAT, A., BHANDARE, S., SANDEL, D., NOÃ©, R., GUY, M. & LAPOINTE, M. (2005) 1.6-b/s/Hz 160-Gb/s 230-km RZ-DQPSK polarization multiplex transmission with tunable dispersion compensation. IEEE Photonics Technology Letters, 17, 495-497

[13] MU, R. M. & MENYUK, C. R. (2001) Symmetric slope compensation in a long-haul WDM system using the CRZ format. IEEE Photonics Technology Letters, 13, 797-799.

[14] SCHUBERT, C., DERKSEN, R. H., MOLLER, M., LUDWIG, R., WEISKE, C. J., LUTZ, J., FERBER, S., KIRSTADTER, A., LEHMANN, G. & SCHMIDT-LANGHORST, C. (2007) Integrated 100-Gb/s ETDM Receiver. Lightwave Technology, Journal of, 25, 122-130.

ISSN: 2277-9655
Impact Factor: 1.852

[15] SUPRADEEPA, V. R., LONG, C. M., LEAIRD, D. E. & WEINER, A. M. (2010) Fast Characterization of Dispersion and Dispersion Slope of Optical Fiber Links Using Spectral Interferometry With Frequency Combs. Photonics Technology Letters, IEEE, 22, 155-157.

[16] TAGA, H. & CHUNG, W. H. (2010) Impact of dispersion map design upon transmission performance of long-haul RZDPSK system using dispersion flattened fiber. Optics Express, 18, 8332-8337.

[17] TAKIGUCHI, K., KAWANISHI, S., TAKARA, H., HIMENO, A. & HATTORI, K. (1998) Dispersion slope equalizer for dispersion shifted fiber using a lattice-form programmable optical filter on a planar lightwave circuit. Journal of Lightwave Technology, 16, 1647-1656.

[18] WANG, K., LI, J., DJUPSJOBACKA, A., CHACINSKI, M., WESTERGREN, U., POPOV, S., JACOBSEN, G., HURM, V., MAKON, R. E., DRIAD, R., WALCHER, H., ROSENZWEIG, J., STEFFAN, A. G., MEKONNEN, G. G. & BACH, H. G. (2010) 100 Gb/s complete ETDM system based on monolithically integrated transmitter and receiver modules. Optical Fiber Communication (OFC), collocated National Fiber Optic Engineers Conference, 2010 Conference on (OFC/NFOEC).

[19] XUEJUN, L., YAOJUN, Q. & YUEFENG, J. (2010) Inline dispersion compensation effect for 100GB/S PDM-CO-OFDM long-haul transmission systems. Network Infrastructure and Digital Content, 2010 2nd IEEE International Conference on.

[20] ZHANG-DI, H., SU-SHAN, L., FEI, X., XIAO, L., XING-JUN, W. & YAN-QING, L. (2010) Dispersion Enhancement and Linearization in a Dynamic DWDM Channel Blocker. Lightwave Technology, Journal of, 28, 822-827.

Table 1: Detail characteristics of the SSMF and DCF used in the simulation

Fiber type	SSMF	DCF
Attenuation (dB/km)	0.2	0.5
Dispersion coefficient (ps/(nm·km))	16.75	–100
Dispersion slope (ps/(nm^2·km))	0.075	–0.35
PMD coefficient (ps/$\sqrt{\text{km}}$)	0.5	0.5
Differential group delay (ps/km)	0.2	0.2
Effective area (μm^2)	80	12

Table 2: Dispersion maps

Dispersion map No.	Pre-dispersion compensation		Post-dispersion compensation	
	(%)	(km)	(%)	(km)
1	0	0	100	16.75
2	10	1.675	90	15.075
3	20	3.35	80	13.4
4	30	5.025	70	11.725
5	40	6.7	60	10.05
6	50	8.375	50	8.375
7	60	10.05	40	6.7
8	70	11.725	30	5.025
9	80	13.4	20	3.35
10	90	15.075	10	1.675
11	100	16.75	0	0

ISSN: 2277-9655
Impact Factor: 1.852

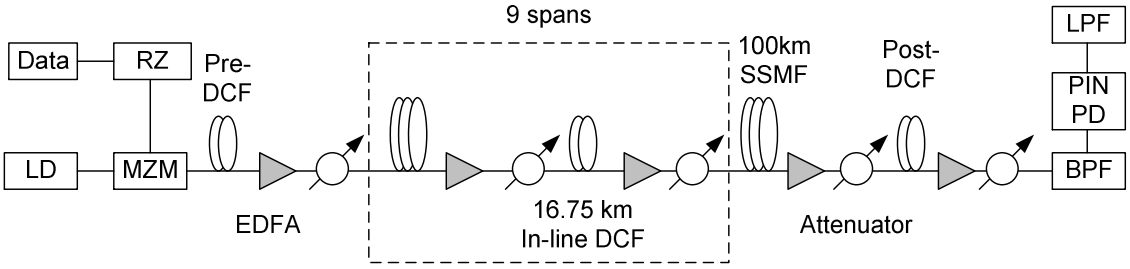

Figure 1: A schematic diagram of the transmission model

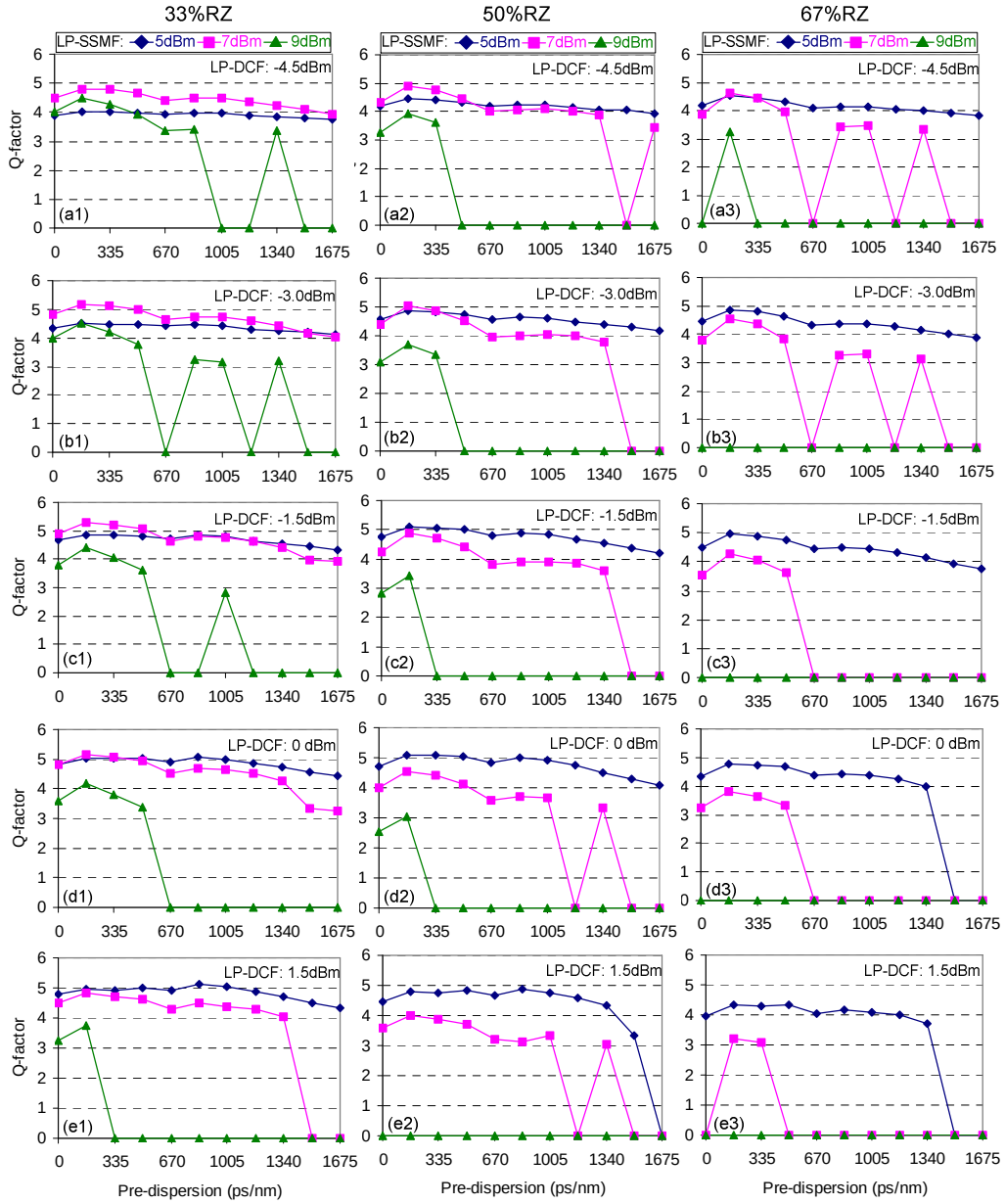

Figure 2: Q-Factor as a function of dispersion map for different launched powers into DCF and SSMF for 33%, 50%, and 67% RZ duty-cycles.

ISSN: 2277-9655
Impact Factor: 1.852

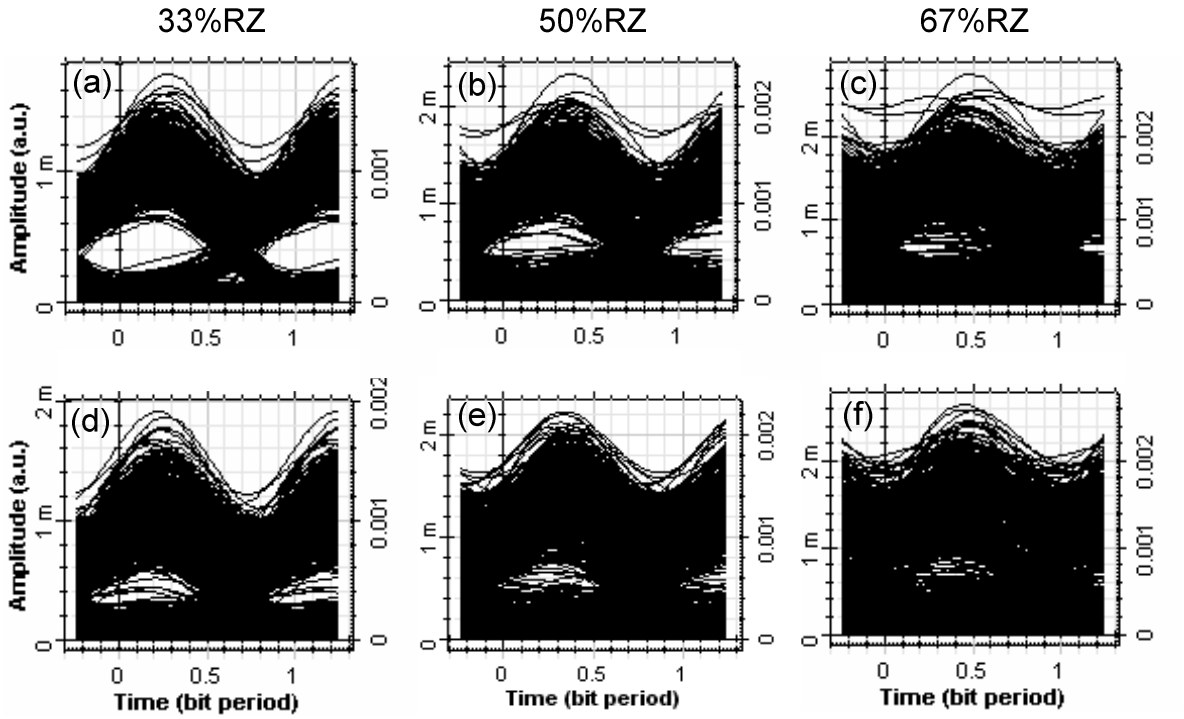

Figure 3: Eye diagrams (a), (b), and (c) 10% pre-compensation for 33%, 50% and 67% RZ, respectively; (d), (e), and (f) 40%, 30%, and 20% pre-compensation for 33%, 50% and 67% RZ, respectively.